Extracting Cloud Motion from Satellite Image Sequences

Remus BRAD and Ioan Alfred LETIA

"Lucian Blaga" University of Sibiu
Computer Science Department
Bulevardul Victoriei 10, 2400 Sibiu, Romania
rbrad@jupiter.ulbsibiu.ro

Technical University of Cluj Napoca
Computer Science Department
Str. Gh. Baritiu 26-28, 3400 Cluj-Napoca, Romania
Ioan.Alfred.Letia@cs.utcluj.ro

Abstract

This paper present a new technique for the estimation of cloud motion, using a sequence of infrared satellite images. It can be considered a challenging task due to the complexity of phenomena implied, as non-linear events and a non-rigid motion. In this circumstances most motion models are not suitable and new algorithms have to be developed. We propose a novel method, combining an Automatic Multilevel Thresholding for image segmentation, a Block Matching Algorithm (BMA) and a best candidate block search along with a vector median regularization.

1 Introduction

Satellite imagery all ready became a common tool for both meteorologists and scientists. A single frame image even if provided in multi-spectral, offers a limited information concerning the evolution of implied phenomena. Furthermore, visible images are available only during daylight, restraining the possibility of a 24-hour analysis. Thus, infrared and water vapour channels are take into account. Due to the dynamical nature of meteorological aspects, an image time sequence analysis is more appropriate. Most of the satellites placed on geostationary orbit are offering half-hourly images in all three spectral channels [1]. The sequence resulting by collecting successive images could be used for cloud motion detection.

As we previously discussed, the infrared image is the only one employed for continuous cloud motion tracking. However, as presented by various authors [2] [3], infrared images could contain artifacts due to the integration effect of imaging sensors. The response of the elementary pixel is the average temperature of all objects present on the corresponding elementary surface. This could be the cause of misclassification errors for different type of clouds.

Segmentation and cloud classification is an essential issue, as well before the computation of motion vectors, as for the identification of different types of meteorological phenomena. The classification methods vary, starting from the use of neural networks, such as Self-Organizing Maps tuned by the Learning Vector Quantization and capable of unsupervised tasks [4] or the Hopfield neural network [5]. The Discrete Karhunen-Loeve transformation is performing classification as well as characterization of cloud elevations in [6] and a Markovian model is used in a labelling scheme for the detection of low height clouds by [2]. Focused on extracting specific features, some authors are employing stereo images in estimation of cloud-top height [7] or convection phenomena [8].

The estimation of cloud motion field is a straightforward objective in the context of image sequence analysis and highly valuable for meteorological and climate applications. However, the automatic extraction of motion is a difficult problem due to the non-linear phenomena of cloud formation and the specific nature of cloud fluid motion. Nearly all-previous work in motion analysis is based on the rigidity assumption, that objects do not change their shape from a frame to another. Generally, this is not the case of many real world examples such as clouds. Consequently, an affine motion model [9] or a non-rigid motion model is defined and fitted using a least-square method [10] in order to retrieve cloud-top heights and winds of hurricane sequences. Other approaches are using a polynomial displacement function to model the local deformation of cloud surface [11] or a vortex type model [3].

Widely used algorithms based on template matching and other similarity metric do not overcome the semi-fluid behavior of clouds and could not be utilized without adaptation. One approach uses the relaxation labelling to refine multiple candidate matches found by template matching [12].

The method presented in this paper is focused on cloud motion detection using Block Matching Algorithm (BMA) combined with a best candidate block search. In order to restrain the search process, we pre-segment the scene using multiple thresholds and extract cloud regions. The rest of the paper is organized as follows: in section 2 the Automatic Multilevel Thresholding and in section 3 the BMA and some speed-up observation are presented. Section 4 describes the best candidate search algorithm and the results are shown in section 5.

2 Automatic Multilevel Thresholding

Identifying multiple object classes can be a problem for unsupervised segmentation algorithms. For the particular case of satellite images, the homogenous regions can be discriminated by a multilevel thresholding. Being a non-parametric method, the Maximum Entropy Criterion (MEC) [13], provides an unsupervised solution to the choice of threshold dilemma.

Consider *I(x,y)*, an image of *NxN* pixels and *m* gray levels. Assume that $G_m=\{0,1,...,(m\text{-}1)\}$ are the gray levels and $f_i\in G_m$ the appearance frequency of the gray levels in image *I*. The probability of *i*th level in image *I*, will be:

$$p_i = \frac{f_i}{N \times N}, i \in G_m \qquad (1)$$

Thus, we obtain the $\{p_i \mid i \in G_m\}$ distribution. For a given *s* gray level, if $0 < \sum_{i=0}^{s-1} p_i < 1$, the next two distributions may be derived from this one, after a normalization:

$$A = \left\{ \frac{p_0}{P(s)}, \frac{p_1}{P(s)}, ..., \frac{p_{s-1}}{P(s)} \right\}$$
$$B = \left\{ \frac{p_s}{1-P(s)}, \frac{p_{s+1}}{1-P(s)}, ..., \frac{p_{m-1}}{1-P(s)} \right\} \qquad (2)$$

where $P(s) = \sum_{i=0}^{s-1} p_i$ is the total probability till (*s-1*) gray level.

The basic idea of the MEC method is the appropriate choice of threshold that maximize the amount of information obtained from the object and background. Recalling that the measure of information is the entropy, the total amount of information given by *A* and *B* is:

$$TE(s) = E_A(s) + E_B(s) = -\sum_{i=0}^{s-1} \left(\frac{p_i}{P(s)} \right) \ln\left(\frac{p_i}{P(s)} \right)$$

$$= -\sum_{i=s}^{m-1} \left(\frac{p_i}{1-P(s)} \right) \ln\left(\frac{p_i}{1-P(s)} \right)$$
$$= \ln[P(s)(1-P(s))] - \frac{H(s)}{P(s)} - \frac{H'(s)}{1-P(s)} \qquad (3)$$

where:

$$P(s) = \sum_{i=0}^{s-1} p_i \qquad H(s) = -\sum_{i=0}^{s-1} p_i \cdot \ln(p_i)$$
$$H'(s) = -\sum_{i=s}^{m-1} p_i \cdot \ln(p_i) \qquad (4)$$

The Maximum Entropy Criterion assumes finding the threshold *s'* that maximizes the following measure:

$$TE(s') = \max_{s \in G_m} TE(s) \qquad (5)$$

If we consider the variances of the two distributions A and B:

$$s_A = \sum_{i=0}^{s-1} (i-m_A)^2 \frac{p_i}{P(s)},$$
$$s_B = \sum_{i=s}^{m-1} (i-m_B)^2 \frac{p_i}{1-P(s)} \qquad (6)$$

where

$$m_A = \sum_{i=0}^{s-1} i \frac{p_i}{P(s)}, \quad m_B = \sum_{i=s}^{m-1} i \frac{p_i}{1-P(s)} \qquad (7)$$

are the mean of A and B, choosing the distribution with the largest variance and applying the MEC to it, one can dichotomize the selected distribution into two more. Hence, the original image can be partitioned in three classes, but the process can continue till the desired number of classes is obtained. Depending of the image contents, we have used 2 or 3 thresholds and managed to segment low level clouds, high level clouds and land or sea.

The method is computationally feasible and leads in short time to the solution. Also, thresholds are determined automatically. Figure 1 shows the original and the segmented images using 2 and 3 thresholds. The test sequence contains infrared images from GOES-W.
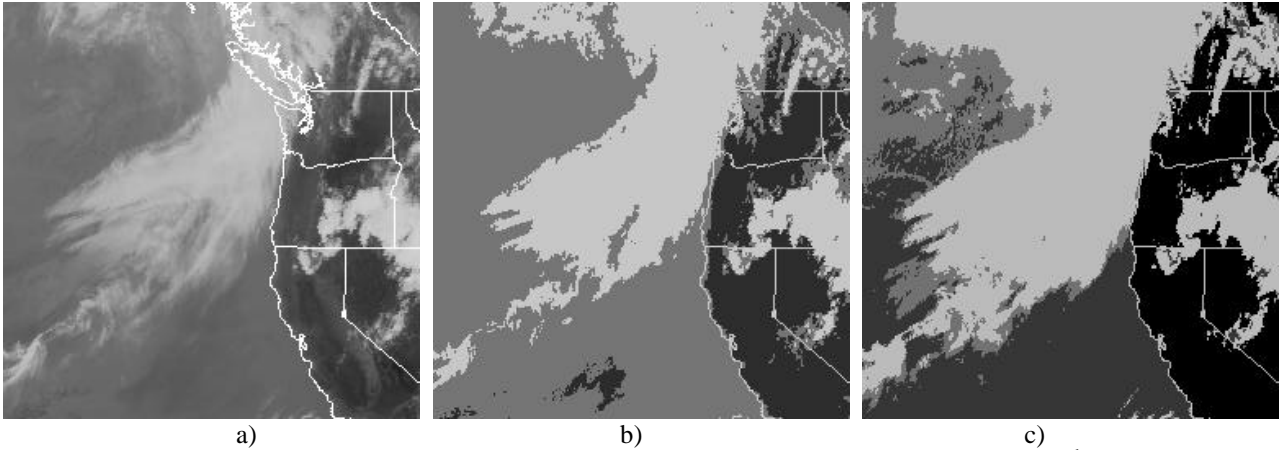

a)   b)   c)

Figure 1. Results of the segmentation using the MEC thresholding. a) the original image,taken on 14th of August 2001 0100Z; b) two thresholds; c) three thresholds

3 Improved Block Matching Algorithm

BMAs are the most common motion estimation methods and widely adopted by image compression and codification standards (MPEG, CCIT H261/262/263). BMA are assuming the fact that a block of pixels has the same translation motion from one frame to another [14]. This is usually applied to a rectangular region of a fixed size. One can define a searching region for the motion vector, such as:

$$|u| \leq \Delta_h \text{ and } |v| \leq \Delta_v \qquad (8)$$

If the block size is K lines and L columns, the searching space is $(K+2\Delta_h)(L+2\Delta_v)$ and the number of possible directions is $(2\Delta_h+1)(2\Delta_v+1)$. Usually, the matching criterion to be optimized is the absolute mean difference of displaced frames:

$$(\hat{u},\hat{v}) = \underset{\substack{(u,v)\in Z^2 \\ |u|\leq\Delta_h, |v|\leq\Delta_v}}{\arg\min} \sum_{i=0}^{K-1}\sum_{j=0}^{L-1}|I_{FD}(i,j;u,v)| \qquad (9)$$

where the frame difference is:

$$I_{FD}(i,j;u,v) = I(i,j;t) - I(i-u,j-v;t-1) \qquad (10)$$

The current window is divided in several rectangular blocks. For each block in the current frame, a displacement vector is obtained. Its coordinates are the best matching block in the search window of the next frame. The Full Search (FS) algorithm is the most common BMA. It requires $(2d+1)^2$ operations and it finds the optimal motion vector among all candidates. Thus, computing complexity makes it useless for real time applications. The aim of reducing the search complexity is achieved by several FS derivations such as: Three Steps Search, 2D Logarithmic Search [15], Cross Search, Orthogonal Search, Four Steps Search [16], Gradient Descend Search.

In our previous work [17], we have derived an improved BMA, by making some comments on the matching process. We have observed the possibility of improving the convergence, using a series of additional tests and a smoothing effect employing an intrinsic optical flow regularization method. Although robust in most cases, for satellite images, the motion vectors retrieved by the mentioned method are not acceptable, as shown in section 5. Due to semi-fluid behavior of cloud motion, the matching process needs to be improved. We have extended the search for the best match candidate over all images in the sequence and proposed a new criterion.

In order to reduce the computational effort and focus on the regions of interest, the images in the sequence are first segmented using the MEC thresholding and clouds regions are extracted. The BMA is applied only on the clouds image portions.

4 Best Candidate Block Search

The Full Search BMA finds the best match between the two blocks of successive frames without any regard to the future evolution of the block or of the block neighborhood. It also offers at the end of the matching process, a list of candidates with their corresponding scores, S_c. We have restricted the list to a predefined number of candidates, usually three or four.

Considering all N images in the sequence, the BMA is applied to the first N-1 images. For each search window in the nth image, a list of first c candidates is saved along with their scores computed with (10). For each start block, a tree is set up. A tree node is storing the following items: - links to child nodes; - candidates list; - candidates score; - vector distance list.

Due to the motion similarity of the neighborhood, we have considered the distance [18] between the block and candidates motion vectors, defined based on the L_2-norm:

$$\left\|\hat{V} - V_i\right\|_{L_2} = \sqrt{(\hat{u}-u_i)^2 + (\hat{v}-v_i)^2} \qquad (11)$$

The distance list is consisting of values computed using (11). For each candidate block, the difference between the two vectors C_c is saved and employed in the search process. The tree arches are assigned a cost based on the resemblance of considered blocks but also on their motion. Therefore, we have considered a weighted sum defined as:

$$Cost = p \cdot S_c + (1-p)C_c \qquad (12)$$

where the weight p is balancing the two factors significance.

The best candidate search algorithm starts with blocks on the first image partition. For each block, a list of path costs is build based on all possible paths starting from it and summing arch costs. Minimizing the path costs will lead to the best block match:

$$Match = \underset{all candidates}{\min} \sum_{n=1}^{N-1} Cost_{n,c} \qquad (13)$$

In the aim of smoothing, a motion vector regularization method is required. We have chosen to apply the vector median filtering [17]. In other cases, each motion vector is replaced by the vector median of the set given by the vector itself and its eight neighbor vectors.

Based on observations, we have adapted the above rule for the candidate search process. In our algorithm, each block has a match candidate and further, each of his

eight neighbors has their own candidates. We apply the above-mentioned rule to the block candidate and neighbor candidates, choosing the candidate most similar to the median vector. The resulted motion field is smoothed as shown in the following section.
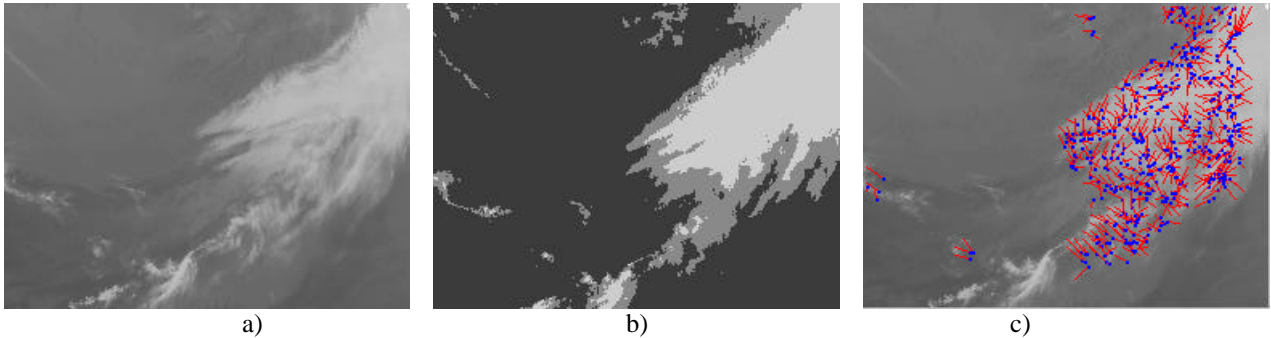

| a) | b) | c) |

Figure 2. Results of the BMA without any improvements. a) The first image, taken on 14th of August 2001 0100Z; b) segmented image; c) motion vectors recovered from the sequence

5 Results

Results are presented using infrared images of GOES-W satellite, take on 14th of August 2001, over the Western Coast of United States. The sequence is composed of five 320x250 images, take at 30 minutes time interval. The block size was 16x16 and the search displacement ±8. The number of candidates was limited to 3 and weight p was chosen 0.8, in the favor of block similarity. Tests have shown that adopting p in [0.6, 0.85] leads to best results, comparing to Full Search.

Figure 2 shows the motion vectors corresponding to the BMA without the best candidate search. A threshold was used to eliminate the vectors of static or low motion blocks. Most of the flow is correct, but matching errors also occurs.

The best candidate search method was then applied and the recovered motion is shown in figure 3a). The vectors are still rough and the median vector regularization is then used in the algorithm creating the smoothed motion field in figure 3b). The final result is a smoothed and distinct motion field suitable for further processing.

The image motion segmentation is straightforward and may be used for meteorological purposes. In the absence of ground data or other sources of cloud motion, validation of the motion field is based on visual perception and manual analysis of the image sequence.
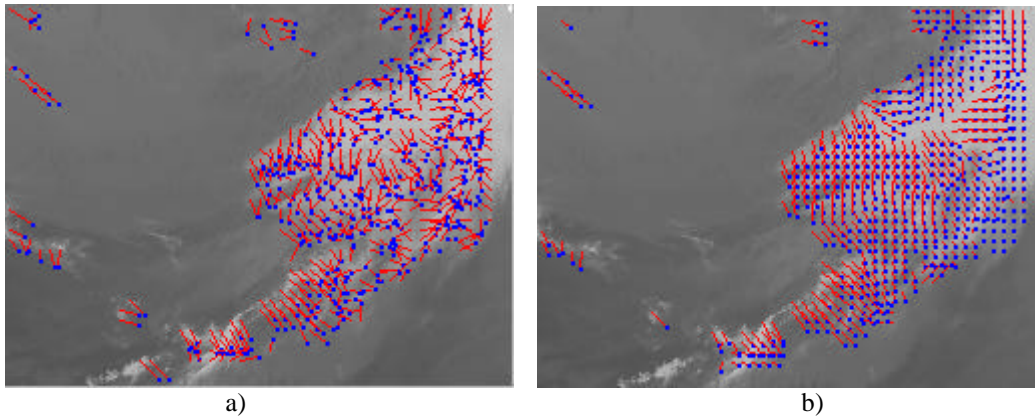

| a) | b) |

Figure 3. Results of the best candidate search method; a) without median vector regularization and b) with vector regularization

6 Conclusions

We have proposed an improved BMA for cloud motion detection. Although speculative, the best candidate search method combined with the vector median regularization can provide very encouraging results. Employing an Automatic Multilevel Thresholding method, we have managed to segment clouds from the satellite image and improved the search process. On infrared satellite images, our approach produces a clear and smoothed motion field, allowing the recovery of cloud motion and the identification of cloud formations.

Further work will involve extensive identification and classification of clouds (precipitation producing low-level clouds) and the analysis of motion convective situations.

References

[1] Eumetsat - "The Meteosat System", *EUM TD 05*, European Organization for the Exploitation of Meteorological Satellites, 2000

[2] Ch. Papin - "Analyse spatio-temporelle d'images satellitaires meteorologiques: detection et suivi de structures nuageuses critiques", *These*, Universite de Rennes I, 1999

[3] D. Bereziat - "Detection et suivi de structures deformables en mouvement, application a la meteorologie", *These*, Universite de Paris XI Orsay, 1999

[4] A. Visa, J. Iivarinen, K. Valkealahti and O. Simula - "Neural Network Based Cloud Classifier", *Proc. International Conference on Artificial Neural Networks*, 1995

[5] S. Cote and A.R.L. Tatnall - "The Hopfield Neural Network as a Tool for Feature and Recognition from Satellite Sensor Images" *International Journal of Remote Sensing*, 18(4), pp.871-885, 1997

[6] C.M. Wittenbrink and G. Langdon - " Feature Extraction of Clouds from GOES Satellite Data for Integrated Model Measurement Visualization", *Proceedings of SPIE/IS&T Conference: Image and Video Processing IV*, vol. 2666, pp. 212-222, San Jose, 1996

[7] D. Poli, G. Seiz and M. Baltsavias - "Cloud-Top Height Estimation from Satellite Stereopairs for Weather Forecasting and Climate Change Analysis", *International Archives of Photogrammetry and Remote Sensing*, vol.XXXIII, part B7/3, pp. 1162-1169, Amsterdam 2000

[8] K. Palaniappan, Y. Huang, X. Zhuang and A.F. Hasler - "Robust Stereo Analysis", *Proceedings of the IEEE International Conference on Computer Vision*, pp.175-181, 1995

[9] L. Zhou, C. Kambhamettu and D.B. Goldgof - "Extracting Nonrigid Motion and 3D Structure of Hurricanes from Satellite Image Sequences without Correspondences",

[10] L. Zhou, C. Kambhamettu and D.B. Goldgof - "Structure and Nonrigid Motion Analysis of Satellite Cloud Images", *ICVGIP'98*, pp. 285-291, December 1998

[11] C. Kambhamettu, K. Palaniappan and A.F. Hasler - "Automated Cloud-Drift Winds from GOES Images", *SPIE Proc. on GOES-8 and Beyond*, Denver, CO, Aug. 7-9, vol. 2812, pp. 122-133, 1996

[12] A.N. Evans - "Cloud Tracking Using Ordinal Measures and Relaxation Labelling", *IEEE Proceedings of International Geoscience and Remote Sensing Symposium*, vol. 2, pp. 1259-1261, 1999

[13] J.C. Yen, F.J. Chang, S. Chang, "A New Criterion for Automatic Multilevel Thresholding", *IEEE Transactions on Image Processing*, vol. 4, no. 3, pp. 370-378, 1995

[14] C.K. Cheung, L.M. Po – "Hybrid Search Algorithm for Block Motion Estimation", *Proc. IEEE Int.Symp.Circ.and Syst.*, vol.IV, pp.297-300, May 1998

[15] C.H. Lee and L.H. Chen - "A Fast Motion Estimation Algorithm Based on the Block Sum Pyramid", *IEEE Transactions on Image Proc.*, vol.6, no.11, pp.1587-1591, November 1997

[16] L.M. Po and W.C. Ma – "A Novel Four-Step Seach Algorithm for Fast Block Motion Estimation", *IEEE Transactions on Circuit and Systems for Video Technology*, vol.6, no.3, pp.313-317, June 1998

[17] R. Brad - "Optical Flow Detection Using an Improved Block Matching Algorithm", *Acta Universitatis Cibiniensis*, Technical Series, vol.XLIII, pp.29-32, Sibiu 2001, ISSN 1221-4949

[18] L. DiStefano and E. Viarani - "Vehicle Detection and Tracking Using the Block Matching Algorithm", *Proc. of 3rd IMACS/IEEE*, Athens, Greece, vol.1, pp. 4491-4496, July 1999